Mechanism for the Rotamase Activity of FK506 Binding Protein from Molecular Dynamics Simulations†

Modesto Orozco,‡ Julian Tirado-Rives, and William L. Jorgensen*

Department of Chemistry, Yale University, New Haven, Connecticut 06511-8118

Received June 4, 1993; Revised Manuscript Received September 13, 1993®

ABSTRACT: Molecular dynamics (MD) and free energy perturbation (FEP) methods are used to study the binding and mechanism of isomerization of a tetrapeptide (AcAAPFNMe) by FK506 binding protein (FKBP). Detailed structures are predicted for the complexes of FKBP with the peptide in both ground-state and transition-state forms. The results support a mechanism of catalysis by distortion, where a large number of nonbonded interactions act together to stabilize preferentially the twisted transition state. The two most important groups for the catalysis are suggested to be Trp^{59} and Asp^{37}, but several other groups are identified as directly or indirectly involved in the binding and catalysis. However, the structural results do not support the notion that the keto oxygen of the immunosuppressive agents FK506 and rapamycin mimics the oxygen for the twisted peptide bond in the FKBP–transition-state complex.

The isomerization of peptidic bonds is a difficult process with free energy barriers typically being 15–20 kcal/mol (Drankenberg & Forsen, 1971; Larive & Rabenstein, 1993). Most peptides correspond to secondary amides and are found exclusively in the *trans* conformation, which is about 2.5 kcal/mol more stable than the *cis* (Drankenberg & Forsen, 1971). However, the tertiary nitrogen in prolyl residues allows the coexistence of *cis* and *trans* isomers in proteins, which may require interconversion during protein folding. Considering the difficulty of this reaction, and the need for efficient folding mechanisms *in vivo*, the existence of enzymes which catalyze the isomerization of prolylpeptides (peptidylprolyl isomerases (PPIs)) is not surprising. PPIs were first characterized by Fischer and co-workers (Fischer et al., 1984), and since then different studies have demonstrated that these enzymes catalyze the *cis* ↔ *trans* isomerism of prolylpeptides during the folding of various proteins (Fischer & Bang 1985, Bächinger, 1987; Lang et al., 1987; Jackson & Fersht, 1991).

The interest in two PPIs, FKBP (FK506 binding protein) and cyclophilin, increased dramatically after the discovery that they are receptors for the immunosuppressant agents FK506 (Harding et al., 1989) and cyclosporin (Fischer et al., 1989a; Takahashi, et al., 1989). Particularly, FKBP was found to be the receptor for a family of immunosuppressant drugs which includes FK506, rapamycin, and ascomycin. It was demonstrated that the binding of the drugs to the protein yields complexes which inhibit T-cell activation (see Rosen & Schreiber, 1992).

FKBP is a small, and highly conserved cytosolic protein, which was isolated and purified by Schreiber and co-workers (Harding et al., 1989), who also cloned the protein (Standaert et al., 1990), and determined the 3-D structure in solution (Michnick et al., 1991) and in the crystal (van Duyne et al., 1991). Actually, 3-D structures of the protein as well as of the protein bound to FK506 (van Duyne et al., 1991a), rapamycin (van Duyne et al., 1991b), and ascomycin (Meadows et al., 1993) are available. The protein's structure features a five-stranded antiparallel β sheet and a short amphipathic α helix, which partially covers one face of the β sheet. The active site, defined as the region where the protein binds the drugs, is located between the α helix and the β sheet in a hydrophobic pocket formed by the side chains of Trp^{59}, Tyr^{26}, Phe^{46}, Phe^{36}, Phe^{99}, Ile^{56}, Tyr^{82}, and Val^{55}.

Both FK506 and rapamycin bind to FKBP as surrogates of prolylpeptides inhibiting the PPI activity (Schreiber, 1991; Rosen & Schreiber, 1992). The low K_i and the presence of a C9-keto oxygen orthogonal to the pipecolinyl ring suggest that both drugs interact with FKBP as mimics of the transition state for *cis* ↔ *trans* isomerization. The fact that cyclosporin, a potent immunosuppressant drug, was a powerful inhibitor of the PPI activity of cyclophilin led to the speculation that the immunosuppressant effects of these drugs were associated with their inhibition of PPI activity (see Rosen & Schreiber, 1992). This attractive hypothesis was ruled out by two observations: (i) rapamycin and FK506 have very different mechanisms for immunosuppressant activity, although their inhibition of PPI activity is similar (Bierer et al., 1990a), and (ii) the analog 506BD is a strong inhibitor of FKBP but is not an immunosuppressant (Bierer et al., 1990b). Accordingly, the relationship, if any, between the PPI and immunophilin activities of FKBP and cyclophilin remains to be determined.

The mechanisms for the PPI action of the immunophilins are also obscure. Fischer and co-workers (Fischer et al., 1989b) proposed a mechanism based on the formation of covalent adducts between the peptide and protein. Kofron et al. (1991) suggested an alternative mechanism in which the protonation of the proline nitrogen would facilitate the isomerization process. Other authors (Albers et al., 1990; Harrison & Stein, 1990; Park et al., 1992; Rosen & Schreiber, 1992) have suggested a mechanism based on the preferential stabilization of the transition state by nonbonded interactions (catalysis by distortion). However, the lack of a structure for a complex between an immunophilin and a peptide has limited the experimental characterization of the rotamase mechanism.

In this paper, we present a molecular dynamics (MD) study on the mechanism of peptide isomerization catalyzed by FKBP. Kinetic measurements have been made for *cis* → *trans* isomerization of tetrapeptides (Fischer et al., 1989; Albers et

† This work was supported by NIH Grant GM32136 and a fellowship from the Fullbright Foundation.

* To whom correspondence should be addressed.

‡ On leave from the Department de Bioquímica, Facultat de Química, Universitat de Barcelona, Martí Franquès 1, Barcelona 08028, SPAIN.

® Abstract published in *Advance ACS Abstracts,* November 1, 1993.

0006-2960/93/0432-12864$04.00/0

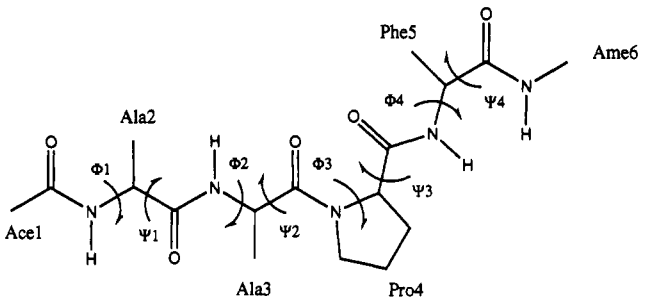

FIGURE 1: Structure and nomenclature of the peptide used in the simulations.

al., 1990; Harrison & Stein, 1990; Kofron et al., 1991; Harrison & Stein, 1992; Park et al., 1992). Consequently, structures for the complexes of a tetrapeptide with a *cis* peptide bond and of its transition state were sought and obtained here. Support for the model includes free energy results for mutation of the P1 residue. Specific interactions responsible for selective stabilization of the transition state are identified. The model clarifies in detail the mechanism of rotamase action and is open to experimental testing. The binding insights should also be useful in the design of high-affinity ligands for FKBP with potential immunosuppressive activity.

COMPUTATIONAL METHODS

A peptide with the sequences Ace-Ala-Ala-Pro-Phe-Ame, where Ace (acetate) and Ame (methylamide) are the N- and C-terminal groups, was used to mimic the natural substrate. Figure 1 shows the structure and related nomenclature; in the following, plain numbering is used for the peptide residues and superscript numbering is used for protein residues. This sequence was selected because is resembles closely the synthetic peptides (Suc-Ala-X-Pro-Phe-pNA) used to measure the activity of PPIs (Fischer et al., 1989; Albers et al., 1990; Harrison & Stein, 1990; Kofron et al., 1991; Park et al., 1992). The peptide was built in both *cis* and *twisted* conformations around the Ala3–Pro4 peptidic bond. The peptide in the *cis* conformation is used as a model of the substrate, and the *twisted* conformation, as a model for the transition state.

The molecular dynamics calculations were carried out with the AMBER program, version 4.0 (Pearlman et al., 1991). The AMBER/OPLS force field (Weiner et al., 1984; Jorgensen & Tirado-Rives, 1988; Jorgensen & Severance, 1990) was used to describe both the peptide and the protein interactions; the only modifications (see Table I) were for the peptidic bond Ala3–Pro4, where the torsional barrier and improper torsion at nitrogen were removed (in both planar and *twisted* conformations), and the bond lengths and angles at N(Pro4) were assigned to average values for planar and twisted amides (Duffy et al., 1992). The stretching and bending parameters related to N(Pro4) were reduced in order to allow the peptide to accommodate easily to the protein environment. Four constraints were used to guarantee that the Ala3–Pro4 peptidic bond stayed in the *cis* or *twisted* conformation. The same force constants were used for both conformers in order to make comparable the Hamiltonians for the *cis* and *twisted* peptides (Table I). The contribution of these constraints to the total energy was not included in any of the simulations.

Standard OPLS Lennard–Jones parameters were used for the *cis* and *twisted* structures (Jorgensen & Tirado-Rives, 1988; Jorgensen & Severance, 1990). Standard OPLS charges for amides were also used to describe the planar structure (Jorgensen & Tirado-Rives, 1988), while the charges for the

Table I: Force Field Parameters for the Ala3–Pro4 Peptide Bond[a]

bond or angle	equil. value	force constant
C–NW	1.39	100
C–NW–CH	115.0	5
C–NW–CQ	115.0	5
CH–NW–CQ	114.0	5

dihedral angle	equil. value	force constant
Cα(A3)–C(A3)–N(P4)–Cα(P4)	120/0	200
O(A3)–C(A3)–N(P4)–Cα(P4)	–60/180	200
C(A3)–N(P4)–CD(P4)–Cα(P4)	–120/180	100
Cα(A3)–C(A3)–O(A3)–N(P4)	180/180	100

atom	q (cis)	q (Twisted)
Cα(A3)	0.200	0.340
C(A3)	0.500	0.437
O(A3)	–0.500	–0.457
N(P4)	–0.570	–0.570
Cα(P4), CD(P4)	0.285	0.225

[a] The atom type NW corresponds to N(Pro4) of the twisted conformer; other atom types are from the standard AMBER/OPLS force-field (Weiner et al., 1984; Jorgensen & Tirado-Rives, 1988). Distances are in Å, angles in deg, charges in electrons, and force constants in kcal/mol Å^2, or kcal/mol rad^2. The dihedral parameters are used as constrains to keep the *cis* or *twisted* conformation. Standard AMBER torsional parameters for the Ala3–Pro4 bond are removed.

twisted amide bond were derived from recent calculations on twisted dimethylacetamide (see Table I and Duffy et al. (1992)). These charges correctly reproduce properties of amides in solution, including free energies of hydration (Jorgensen & Tirado-Rives, 1988; Duffy et al., 1992).

The crystal structure of FKBP bound to rapamycin (van Duyne et al., 1991b) was used as a starting point for the calculations. First, the peptide in the *twisted* form was overlaid on rapamycin. The conformation of the peptide was modified by rotation around single bonds to obtain the best fit with rapamycin and to reproduce well the environment of analogous hydrogen bond donor and acceptor groups. Once a suitable conformation of the peptide was obtained, the drug was removed, yielding a protein–peptide complex in which the peptide not only reproduces the general shape of rapamycin but also has a similar pattern of hydrogen bonds with the binding pocket.

The protein–peptide model was solvated with a sphere of 23-Å radius containing TIP3P water (Jorgensen et al., 1983) centered on the center of mass of the peptide. This led, after removal of water molecules with unreasonably short contacts, to a solvation sphere with 1002 water molecules. A soft harmonic term with a force constant of 1.5 kcal/(mol Å^2) was used to retreive water molecules drifting beyond the boundary of the sphere. The resulting system is shown in Figure 2, where it is clear that the sphere of water provides extensive hydration of the binding site for the MD calculations. The solvated system was then divided into two regions: (i) an inner part, which includes the peptide, the water, and all residues which have at least one atom closer than 12 Å to any atom of the peptide, and (ii) an outer part, which contains the rest of the protein. The first part includes 78 residues of the protein and was free to move in all minimizations and MD simulations, while the outer part with 25 residues was kept rigid in all calculations. This initial system was then prepared through 2000 steps of energy minimization (500 where the peptide and the protein were kept rigid, 500 where only the peptide was fixed, and 1000 where the entire system was minimized), and 40 ps of MD for heating from T = 198–298 K and equilibration. The final equilibrated structure was used to run 500 ps of constant temperature MD at 298 K. The

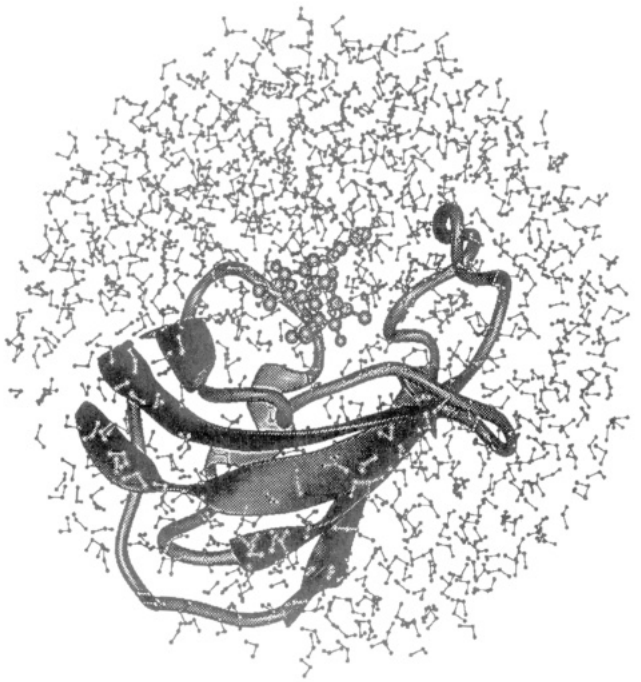

FIGURE 2: FKBP–peptide complex inside the 23-Å sphere of water used in the MD simulations.

integration step was 0.002 ps, and the coordinates were stored every 0.2 ps. SHAKE (Ryckaert et al., 1977) was used to maintain all bonds lengths at their equilibrium values. A nonbonded spherical cutoff of 8 Å and a residue-based nonbonded list, updated every 25 integration steps, were used.

The structure at t = 100 ps was used to generate the *cis* peptide–protein complex. The change between *twisted* and *cis* peptides was done in six steps with the angles of the constraints and the charges gradually modified from *twisted* to *cis* values (Table I). After each change, the peptide alone was optimized *in vacuo* for 100 cycles; harmonic constraints were used to guarantee that most of the conformational changes would occur mainly in the Ala3–Pro4 area. This simple procedure mimics a fast change from *twisted* to *cis*, and we found it to be superior to other methods such as stepwise rotation for the full protein–peptide system and simulated annealing.

The *cis* peptide was then placed inside the binding pocket of the solvated protein occupying the same location as the *twisted* conformer. The system was optimized, heated, and equilibrated during 40 ps using a procedure analogous to that described above. A 500-ps MD trajectory was then run for the *cis* system. It should be noted that the *cis* and *twisted* systems contain the same number of atoms, identical definition of the hydration shell, identical partitioning between the inner and outer regions, and, except for the charges, the same Hamiltonian.

Free energy calculations were used to predict the difference in isomerization rate between two peptides, Ace-Ala-Ala-Pro-Phe-Ame and Ace-Ala-Gly-Pro-Phe-Ame, for comparison with experimental data on the corresponding Suc-Ala-X-Pro-Phe-pNA peptides (Albers et al., 1990; Harrison & Stein, 1992; Park et al., 1992). The thermodynamic cycle in Figure 3 was utilized to obtain the change in free energies of activation. The free energy changes for the Ala3 → Gly3 mutations was computed by statistical perturbation theory according to eq 1 (Zwanzig, 1954). These mutations were started with the structures and velocities of the *cis* and *twisted* systems at the end of the MD runs. The calculations were done in 41 double-

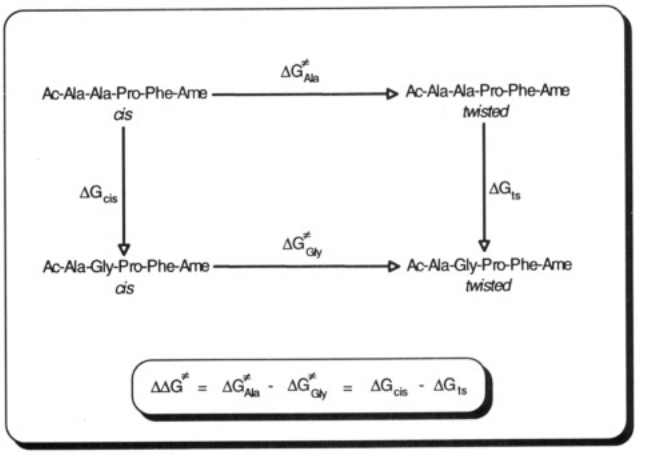

FIGURE 3: Thermodynamic cycle used to determine the $\Delta\Delta G^{\ddagger}$ of isomerization between the Ala and Gly peptides. Dark lines are the peptide and light lines are the rapamycin molecule.

$$\Delta G = \sum_{\lambda_i=0}^{\lambda_i=1-\Delta\lambda} -kT \ln \langle \exp[-(V_{\lambda_i+\Delta\lambda} - V_{\lambda_i})/kT] \rangle_{\lambda_i} \quad (1)$$

wide sampling windows of 5 ps each (2 ps of equilibration and 3 ps of averaging) for a total of 205 ps for each mutation. The entire peptide was considered as the perturbed group in the mutation; not only the intergroup interactions, but also all the intragroup nonbonded interactions (including 1–4) were considered in the evaluation of the free energy changes. We had determined in pilot calculations that the explicit inclusion of bonded contributions in the free energy calculation led to increased noise in the final free energies, but did not alter significantly the final results. The averaging in eq 1 was performed by MD simulations at constant T = 298 K, where T is the temperature, k is Boltzmann's constant, λ is the coupling parameter, which controls the evolution of the Ala → Gly mutation, and V_λ is the potential energy of the system.

A similar simulation was performed to determine whether or not the structure of the *cis* peptide was able to explain experimental binding data (Parker et al., 1992). Thus, the difference in free energy of binding between Ala and Gly (cis)peptides ($\Delta\Delta G_{bind}$) was determined as the difference between the free energy changes in the mutation Ala → Gly in water ($\Delta G_{mut}{}^{water}$), and in the protein complex ($\Delta G_{mut}{}^{prot}$). In order to compute $\Delta G_{mut}{}^{water}$ the Ala (cis)peptide in the conformation adopted inside FKBP at the end of the MD was introduced into a cubic box (edge ≈ 30 Å) of TIP3P water. The closest water molecules were removed to yield to a system with 807 water molecules. The system was minimized for 3000 cycles (2000 with the peptide fixed and 1000 with the entire system free). The system was heated from 198 to 298 K during 5 ps of NVT MD (during the first 3 ps only the water was allowed to move), and equilibrated during 20 ps of NPT MD (T = 298 K; P = 1 atm). The free energy change for the Ala → Gly mutation was computed using 41 double-wide sampling windows of 2.5 ps (1.25 ps of equilibration and 1.25 ps of averaging) for a total of 102.5 ps. Periodic boundary conditions were used in all the simulations. All the remaining technical details of the simulations were identical to those noted above for the peptide–protein complexes.

RESULTS

Transition-State Structure. The structure of the twisted transition state model, which was obtained after the fitting, optimization, and equilibration process resembles the general

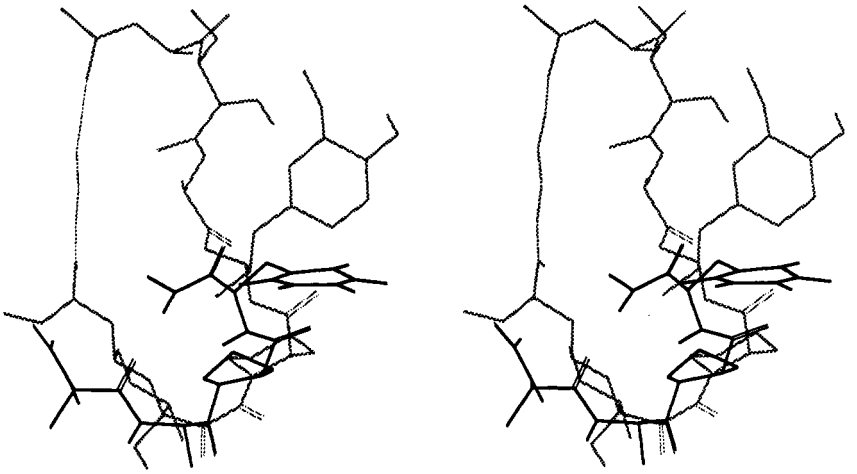

FIGURE 4: Superposition of the structures of bound rapamycin and the *twisted* peptide after the equilibration.

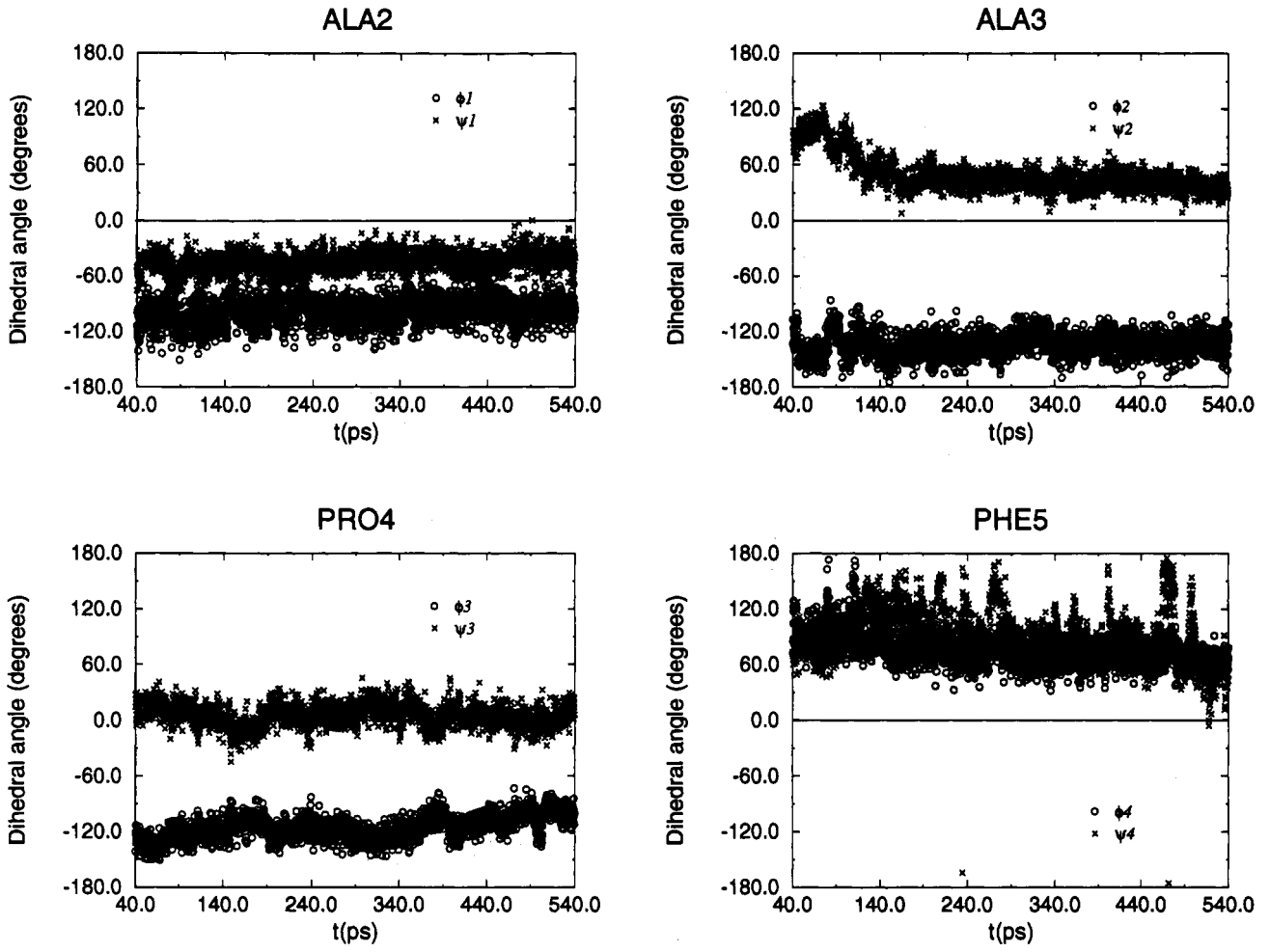

FIGURE 5: Dihedral angle histories for the *twisted* peptide.

structure of rapamycin, as shown in Figure 4. The main chain of both molecules overlaps well, and the H-bond donors and acceptors are also in proximal positions. In particular, O(Ala3) is placed very close to the keto oxygen of rapamycin, and the Pro ring shares the space of the pipecolinyl ring.

Analysis of the 500 ps trajectory shows flexibility in the peptide, especially for the side chain of Phe5 and in the Ala3–Pro4 region. The histories for the main chain dihedral angles shown in Figure 5 reveal that most movements are short range oscillations, which do not lead to dramatic changes in the structure. However, there is also a systematic movement occurring for the Ala3–Pro4 region in the 80–120 ps period, which leads to a significant change in the relative orientation of the peptide inside the protein, as shown in Figure 6. The conformation of the 60 and 540 ps structures are similar, as noted in Figures 5 and 6 with a general "turn" topology stabilized by one or two intrachain hydrogen-bonds. The largest differences between the 60 ps and 540 ps structures are in the positioning of the proline ring and Ala3–Pro4 with respect to the binding site (see Figures 6 and 7). The reduction in ψ for Ala3 after 60 ps secures the hydrogen bonds for the turn structure and leads to better possitioning of the Ala3

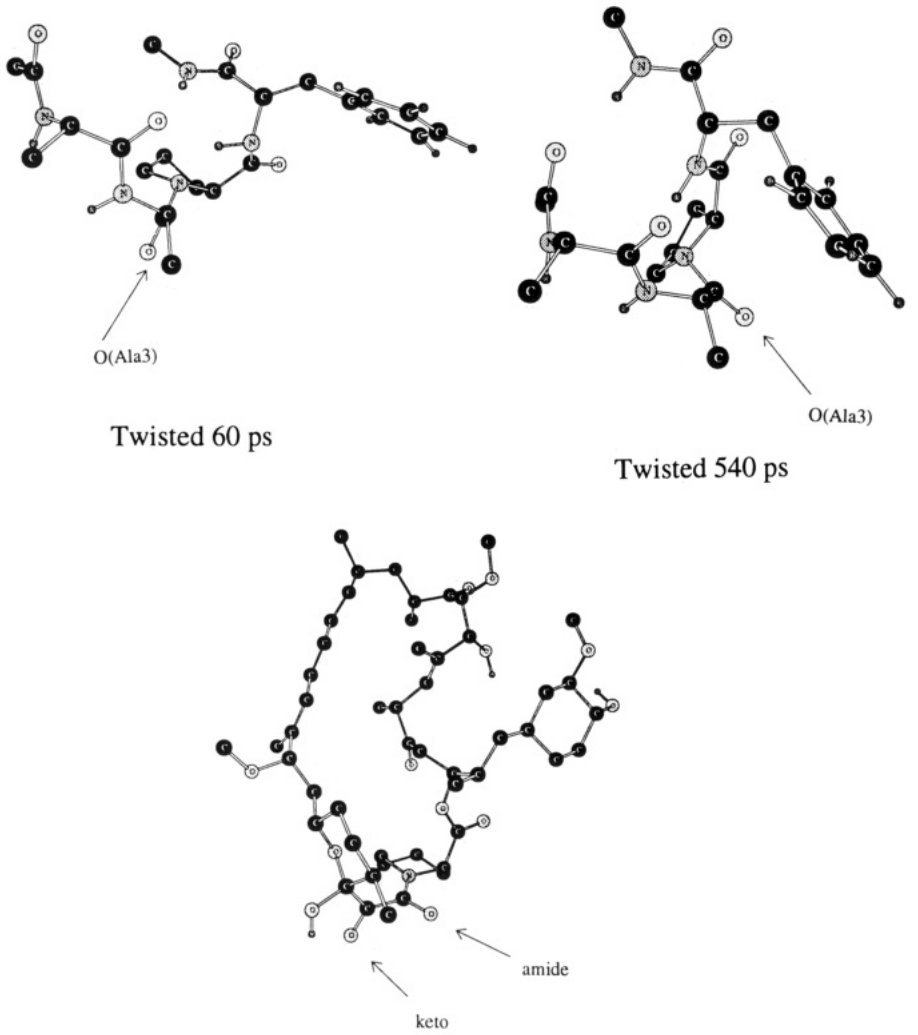

FIGURE 6: Representation of the structure adopted inside the binding site by rapamycin, and the *twisted* peptide at 60 and 540 ps. A common reference axis was used to orient the molecules.

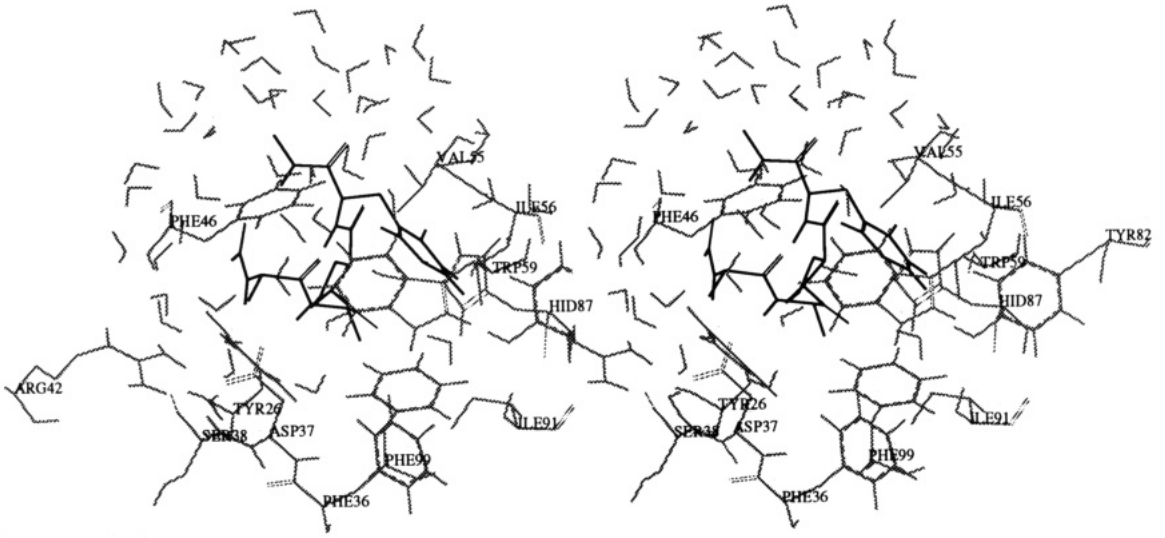

FIGURE 7: The *twisted* peptide bound to the active site of FKBP.

carbonyl group with respect to the Asp[37] side chain (see below).

The distances for key interactions are shown in Figure 8. A hydrogen bond exists between the Asp[37] side chain and the amino groups of Ala2 and often Ala3, which are proximal (Figures 6 and 7). Two intrachain hydrogen bonds are also common: Ame6–Ace1, and Phe5–Ala2, which stabilize the turn structure. Another interesting interaction is the close contact (ca. 2.0 Å) between the amide hydrogen of Phe5 and the N of Pro4. There are no hydrogen bonds between the oxygen of Ala3 and the protein. The analysis of Figure 8

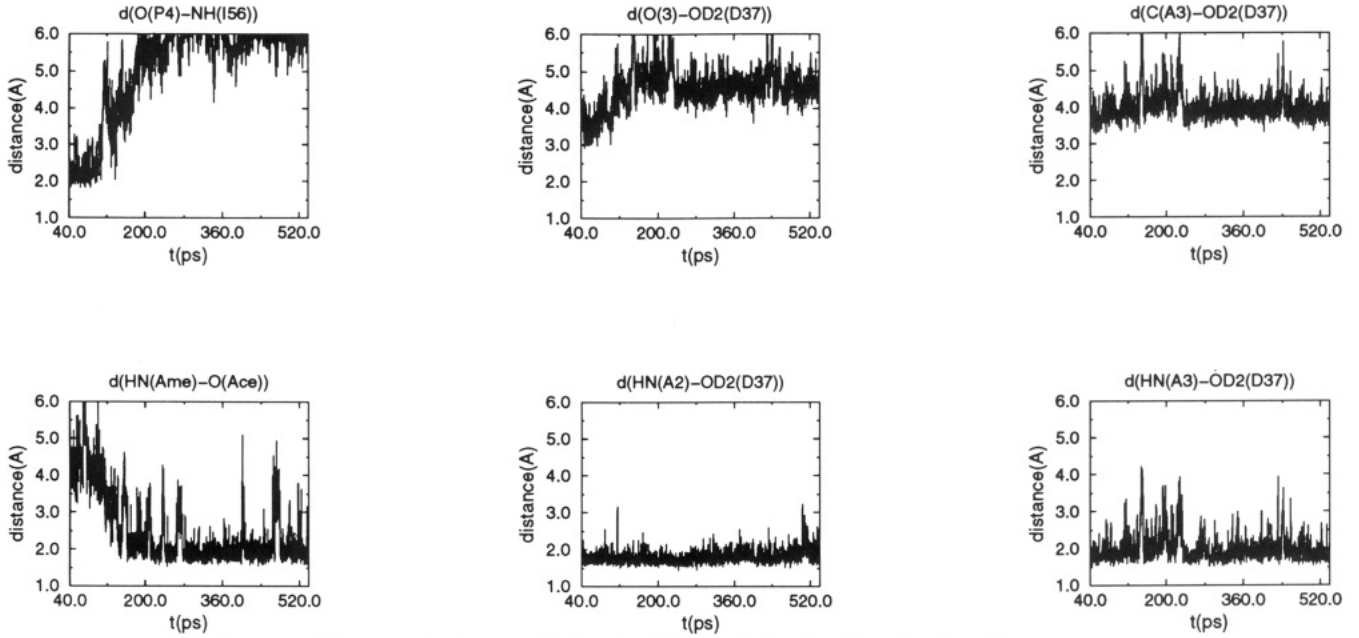

FIGURE 8: Histories for selected interatomic distances during the MD simulation for the *twisted* peptide.

reveals that the movements during the 80–120 ps period have two major consequences: first the hydrogen bond between Ile[56] and Pro4, which mimics one of the hydrogens bonds in the crystal structure of the FKBP–rapamycin complex is lost, and second, the intrapeptide hydrogen bond between Ame6 and Ace1 is formed. Two less dramatic, but particularly significant changes, are in the distances between the Asp[37] side chain and the C=O moiety of Ala3. In the starting conformation, one of the negatively charged oxygens of Asp[37] is about 3.6 Å from O(Ala3) and 4.0 Å from C(Ala3), while in the final conformation these distances are around 4.7 and 3.9 Å, respectively. Thus, the conformational change in the 80–120-ps period transforms a clearly bad charge–dipole contact into a much more favorable one. It is also notable that after the conformational change, *the position of the carbonyl oxygen of Ala3 is more similar to that of the amide oxygen rather than the keto oxygen of rapamycin.*

The movement of the O(Ala3) from the starting to the final conformation leads to a modest reduction in the number of aryl interactions (a contact O(Ala3)–H(aromatic) is considered as an aryl interaction when the O···H distance is less than 3.2 Å) between O(Ala3) and the aromatic side chains of Phe[36], Phe[99], Tyr[26], and Tyr[82] from 2.6 to 2.0. Analysis of the hydration of the peptide used a geometric definition of a hydrogen bond requiring an N···H or O···H distance less than 2.5 Å, and a donor–hydrogen–acceptor angle between 120 and 180°. With this definition, there are initially 5.4 waters hydrogen bonded to the peptide on average. This number increases to 5.8 in the last 240 ps of the trajectory. One water is bound to O(Ala2), 1.3 to O(Ace1), and 1.5 to O(Phe5); however, the latter's intrapeptide hydrogen bonding partner, the amino group of Ame6, is hydrogen bonded to a water only 10% of the time. O(Pro4) is not solvent exposed in the starting conformation where it is H-bonded to Ile[56], but in the final part of the trajectory (100 → 540 ps) it is hydrogen bonded to an average of 1.1 water molecules. Finally, O(Ala3) is in a purely hydrophobic place during the first 320 ps of the trajectory, but at this point, it captures a water molecule, which remains hydrogen bonded during 80% of the remaining time as in Figure 7 (an average of 0.4 water is bound to O(Ala3) when the complete trajectory is considered).

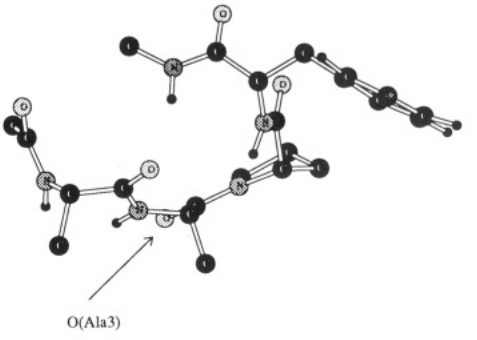

Cis 540 ps

FIGURE 9: Representation of the conformation adopted inside the active site by the *cis* peptide. Only the structure at the end of the MD run is shown, since no major changes occur for the *cis* peptide during the simulation.

The last step in the analysis of the protein–peptide interactions was identifying water bridges connecting polar groups of the peptide and the protein. There is a water bridge between O(Phe5) and the carbonyl of Glu[54] during 55% of the time, mimicking another one of the hydrogen bonds in the FKBP-rapamycin structure. A water bridge is also detected 43% of the time between O(Ala2) and His[87], and one exists 40% of the time in the 120–320-ps period between O(Pro4) and Tyr[82]. The latter bridge is lost in the final part of the MD, when the water on O(Ala3) makes a bridge to the hydroxyl group of Tyr[82] during 80% of the time (Figure 7).

Cis Conformation. The *cis* form of the bound peptide also has a turn structure, with obvious similarities to the structures of rapamycin and the *twisted* peptide (Figure 9). The position of the peptide in the binding site is very similar to that of rapamycin, with the proline ring replacing the pipecolinyl ring. The MD provides significant sampling of the configurational space of the peptide, but no systematic changes occur, as evident in the distributions of main chain dihedral angles shown in Figure 10. Key interactions are indicated in Figures 11 and 12. Thus, the Asp[37] side chain is again hydrogen bonded to the amino group of Ala2, and often to the amino group of Ala3. Hydrogen bonds also form ocasionally between

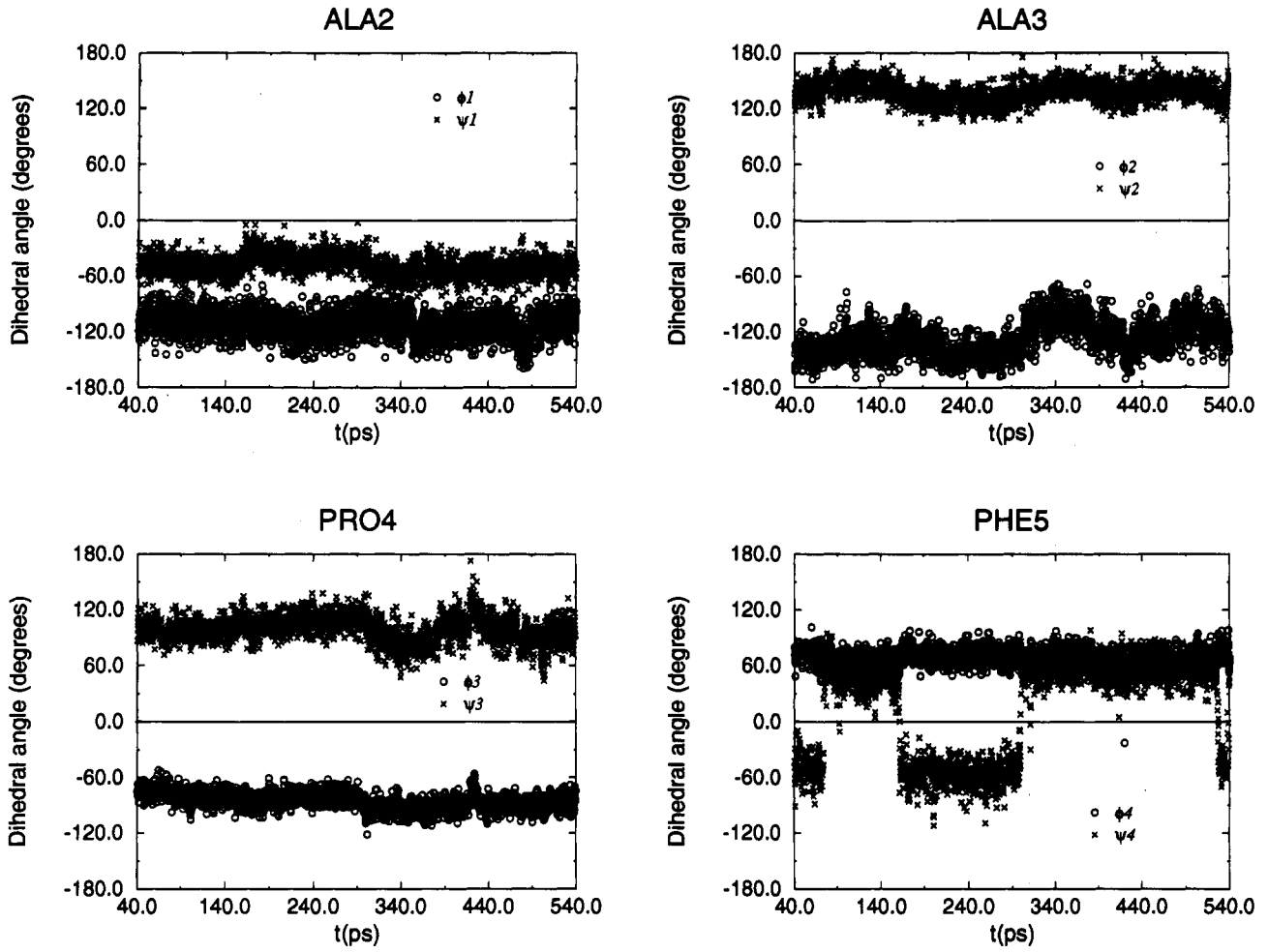

FIGURE 10: Dihedral angle histories for the *cis* peptide.

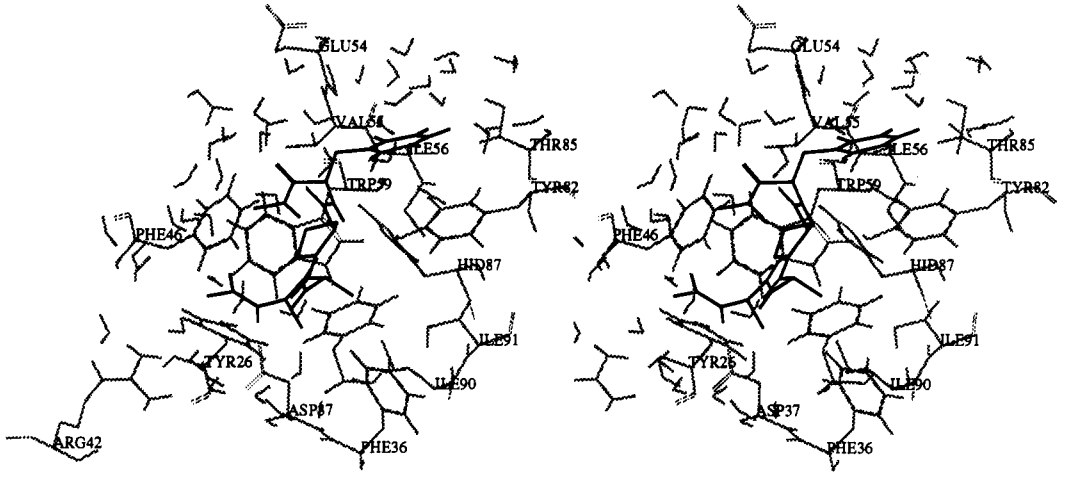

FIGURE 11: The *cis* peptide bound to the active site of FKBP.

NH(Ame) and O(Ala2) and between NH(Phe5) and O(Ala2). Other H-bonds (not shown in Figure 12) that are present some of the time are between NH(Phe5) and the imidazole ring of His[87] and between NH(Ame) and O(Pro4). A hydrogen bond exists between O(Ala3) and the hydroxyl group of Tyr[26] only during short periods of time, for instance in the 160–180-ps period, but most of the time this H-bond is not present. It is very interesting to look at the relative positions of Asp[37] with respect to the carbonyl group of Ala3; the OD2–O(Ala3) distance is around 3.3 Å, and the OD2–C(Ala3) distance is about 4.0 Å. These reveal a repulsive charge–dipole contact, which contrasts the favorable interaction found for the transition state. Intrapeptide hydrogen bonds that are present in the *twisted* conformation, but are not present in the *cis* structure are between NH(Phe5) and N(Pro4) and between NH(Ame) and O(Ace).

The carbonyl oxygen of Ala3 is near the aromatic side chain of Phe[99] and Tyr[26] (Figure 11); the average number of aryl interactions is 1.2 for this oxygen, which is ca. 1 less than in the *twisted* conformation. The *cis* peptide is well hydrated, with an average of 5.0 waters hydrogen bonded (0.4–0.8 less than in the *twisted* structure). A detailed analysis of the hydration shell shows that the oxygens of Ace and Phe5 are the best hydrated, with an average of 1.9 and 1.8 water

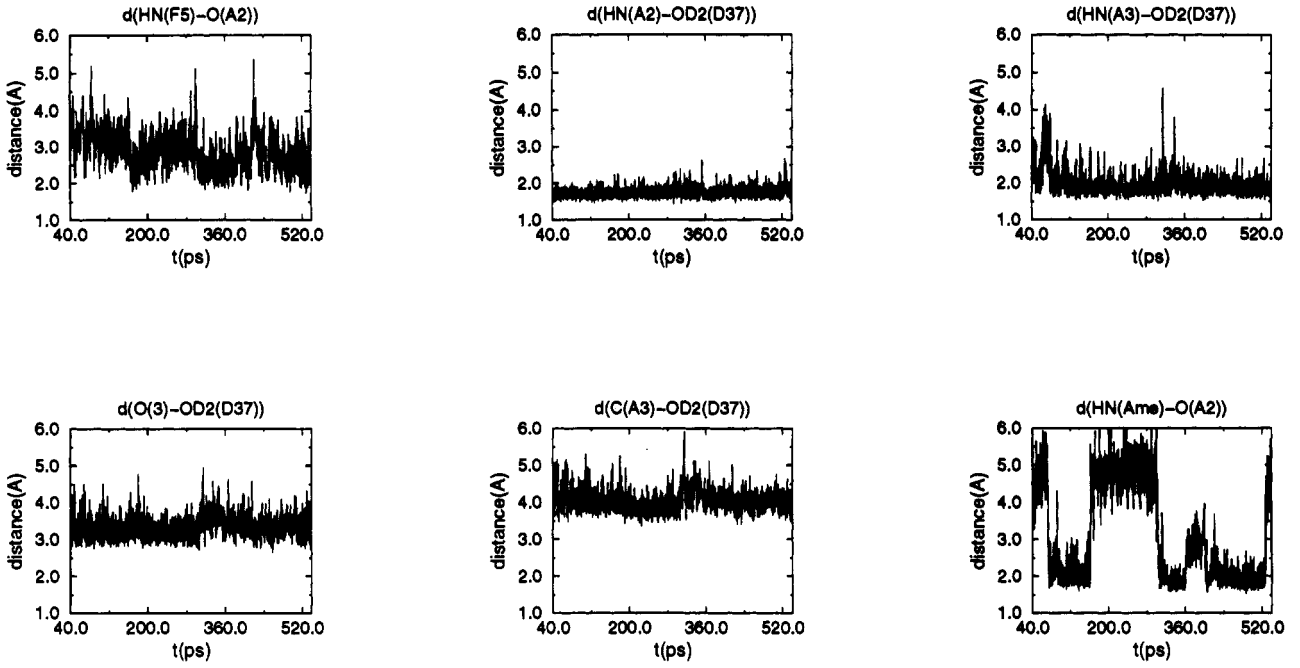

FIGURE 12: Histories for selected interatomic distances during the dynamics for the *cis* peptide.

molecules bound. The oxygens of Pro4 and Ala2 are less well solvated with 0.5 and 0.7 water molecule bound on average. The amino group of Ame is hydrogen bonded to a water only 10% of the time. O(Ala3) which is hydrogen bonded to a water molecule in the last part of the MD for the *twisted* conformer, is not solvated in the *cis* conformation. Three water bridges exist sporadically; the most common involve Glu^{54} which has water bridges with O(Pro4) and O(Phe5) during 31% and 22% of the simulation, respectively. A water bridge between O(Ala2) and the imidazole ring of His^{87} also exists 38% of the time during the first 200 ps, but it is rare in the remaining 340 ps. Finally, there are no water bridges involving Tyr^{82} and O(Pro4) or O(Ala3), in contrast to the *twisted* conformer.

Free Energy Calculations. The structures determined for both the *cis* and *twisted* complexes seem reasonable from the viewpoints of stability, interactions, and function. Nevertheless, doubt remains about whether or not they are the real conformations. Comparison of total potential energies demonstrates that the *twisted* form is slightly lower in energy than the *cis*, in good agreement with the proposed stabilization of the transition state by the enzyme, but the difference (around 7 kcal/mol) is not significant considering the statistical noise in the simulations (±70 kcal/mol). Additional MD calculations, graphical manipulation, and simulated annealing procedures support the correctness of the structures, but it is obvious that more quantitative results are desirable. Though an experimental 3-D structure of the FKBP–peptide complex is not available, attempts could be made to reproduce kinetic data for the isomerization catalyzed by the enzyme. One possibility was to compute the potential of mean force (PMF) for rotation about the Ala3–Pro4 peptidic bond, and to compare the ΔG of this process with the observed ΔG of activation for the enzymatic reaction ($\Delta G^{\ddagger}$). Unfortunately, several attempted PMF calculations using holonomic constrains encountered major technical difficulties. Development of alternative procedures for such perturbations is under consideration.

However, some support can be sought by comparison of the relative $\Delta G^{\ddagger}$ of peptides with different sequence. Park et al. (1992) found a difference in k_{cat} favoring Ala over Gly at the P1 position in the Suc-Ala-X-Pro-Phe-pNA peptide. Their k_{cat} ratio of 1200 (T = 278 K) translates to a lower $\Delta G^{\ddagger}$ for the Ala(P1) peptide by 3.9 kcal/mol. Harrison & Stein (1992) reported a k_{cat}/K_m ratio for Ala and Gly peptides of 44 (T = 283 K), which considering the K_m for these peptides (Park et al., 1992) translates to a lowering of $\Delta G^{\ddagger}$ for the Ala(P1) peptide by 2.7 kcal/mol. Finally Albers et al. (1990) found a k_{enz} ratio between Ala(P1) and Gly(P1) peptides of 12, which considering the K_m values of Park et al. (1992) yields a difference in $\Delta G^{\ddagger}$ of 1.9 kcal/mol (T = 278 K) favoring the isomerization of the Ala(P1) peptide. The Ala → Gly mutation is an attractive one computationally in view of the small structural change, and it was pursued according to the thermodynamic cycle in Figure 3 using 205-ps MD simulations as described above. Exact quantitative comparison between computation and experiment is not available here because of the range of uncertainty of both experimental and theoretical results, of the differences in peptide end groups, and of the temperature. However, the experimental data clearly suggest a significant quantitative preference for the isomerization of the Ace-Ala-Ala-Pro-Phe-NMe peptide over the P1 = Gly one. Accordingly if the models for the *cis* and *twisted* complexes presented above are correct, this qualitative difference should at least be reproduced.

ΔG profiles for the Ala (λ = 10) → Gly (λ = 0.0) mutation in the *cis* and *twisted* peptides are displayed in Figure 13. Both profiles are smooth and do not have discontinuities. This, and the small differences between the "forward" and "reverse" routes support the convergence of the results. The Ala → Gly mutation gives a very small ΔG (–0.2 ± 0.1 kcal/mol) for the *cis* conformer, which means there is only a small change in the strength of the protein–peptide interaction when Ala3 is substituted by Gly. In contrast, the same mutation for the *twisted* conformer leads to a positive ΔG of 1.4 ± 0.1 kcal/mol, indicating that the transition state with an Ala at position 3 interacts better with the protein than the peptide with a Gly. Thus, the FEP calculations predict that the peptide with Ala rather than Gly at position 3 would be isomerized more efficiently by $\Delta\Delta G^{\ddagger}$ = 1.6 ± 0.2 kcal/mol, consistent with the trend in the experimental data. The reasons for this notable difference can be found in the placement of the methyl group

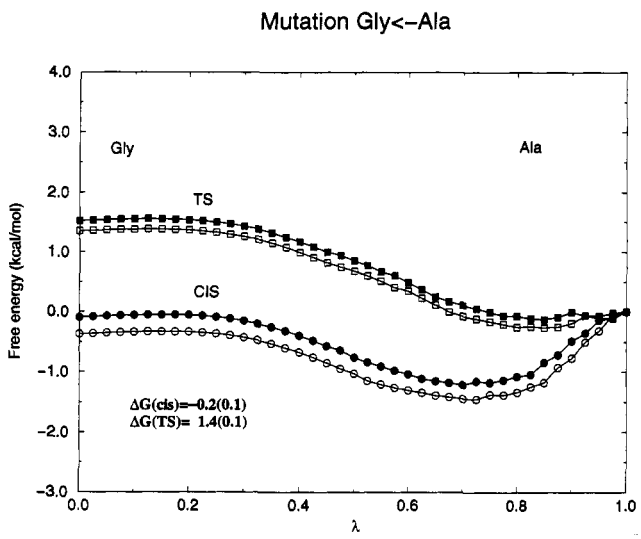

FIGURE 13: Free energy changes during the Ala3 (λ = 1) → Gly3 (λ = 0) mutation. Open symbols are used for the "forward" (λ = 0 → λ = 1) simulations and filled symbols for the "reverse" (λ = 1 → λ = 0) ones.

of Ala3 in the cis and twisted conformations (see Figures 7 and 11). In both cases, the methyl group is placed in a large hydrophobic pocket (able to contain a Leu side chain) defined by the side chains of Tyr^{26}, Phe^{36}, Ile^{90}, Ile^{91}, Leu^{97}, and Phe^{99}. Nevertheless, detailed inspection (see Figures 7 and 11) shows that the methyl group is deeper inside the pocket in the *twisted* conformation than in the *cis*. As a consequence, when the methyl of Ala3 in the *twisted* conformation disappears during the mutation, a hole in the hydrophobic pocket appears. This leads to a concerted displacement of the proline ring and the side chain of Trp^{59}, yielding a less stable structure for the protein–peptide complex. Such a movement does not occur in the *cis* peptide, in which case the methyl group is not as deep into the hydrophobic pocket.

DISCUSSION

The peptide Ace-Ala-Ala-Pro-Phe-Ame binds well to the active site of FKBP in both the *cis* and *twisted* conformations, as evident in the fact that after 540-ps trajectories the peptide remained in the active pocket, without any apparent tendency to leave. The active site, defined by residues with atoms closer than 5 Å to any atom of the peptide is formed by (see Figures 2, 7, and 11): Tyr^{26}, Phe^{36}, Asp^{37}, Ser^{38}, Arg^{42}, Phe^{46}, Glu^{54}, Val^{55}, Ile^{56}, Trp^{59}, Tyr^{82}, Thr^{85}, His^{87}, Ile^{90}, Ile^{91}, Leu^{97}, and Phe^{99}. It is interesting to note the large number of aromatic and hydrophobic residues (Rosen & Schreiber, 1992). The active site is quite large (see Figures 7 and 11), with the Trp^{59} indole at the end. An arbitrary coordinate system can be defined, when looking from the outside toward Trp^{59}, Tyr^{82} is on the right, and Tyr^{26} is on the left (see Figures 7 and 11). According to this reference system, two hydrophobic regions can be located, one at the top formed by Phe^{46}, Val^{55}, and Ile^{56} and the other at the bottom formed by Phe^{36}, Ile^{90}, Ile^{91}, Leu^{97}, and Phe^{99}. Several polar groups are located perpendicular to these two apolar regions, His^{87} and Tyr^{82} on the right, and Tyr^{26}, Asp^{37}, and Arg^{42} on the left. The peptide adopts a turn structure in both conformations, the proline ring being the center of the turn and the group deepest inside the active site. The terminal groups, Ame and Ace, are mostly exposed to solvent, which suggests that a tetrapeptide is the elemental unit which interacts with the protein. The carbonyl group of Ala3 is in different positions in the *cis* and *twisted* peptides. Thus, it is pointing toward the Asp^{37} side chain for the *cis* peptide, while in the *twisted* conformation it is pointing in the opposite direction. The side chain of Ala3 is located in a large, very hydrophobic pocket at the bottom of the active site. Graphical manipulations, and molecular mechanics calculations demonstrate that this hydrophobic pocket can easily accommodate a bigger residue at position 3 like Leu.

As noted above, both the *cis* and *twisted* peptides adopt a turn structure. This is consistent with the general conformation of inhibitors of the protein like FK506 and rapamycin and with the marked tendency of proline to occur in turns. Different conformations might be obtained for peptides with other sequences; however, the general conformational characteristics of substrate peptides, especially near the Pro region, may be expected to be similar to those described above.

The structural results make a mechanism involving covalent adducts unlikely (Fischer et al., 1986b). Any potential nucleophiles like Cys and Ser are in general far from the Ala3–Pro4 peptidic bond. The protonation of N(Pro4) by an acidic group of the protein (Kofron et al., 1991; Harrison & Stein, 1990) also seems improbable owing to the lack of acidic groups close to N(Pro4). A possible hydrogen bond between N(Pro4) and a group of the protein (Kofron et al., 1991) was not detected during the simulations, but a short intrachain contact between HN(Phe5) and N(Pro4) exists almost all the time for the *twisted* conformation, and may contribute to stabilize the transition state *via* "enzyme-induced autocatalysis". In summary, our results support a mechanism of catalysis by distortion (Albers et al., 1990; Harrison & Stein, 1990; Park et al., 1992; Rosen & Schreiber, 1992), where different non-bonded interactions act in concert to stabilize the transition state preferentially over the substrate. It may be noted that the reduction in the $\Delta G^{\ddagger}$ of isomerization of a peptide, like that considered here, due to the action of FKBP is 6–7 kcal/mol from experimental rate data (Park et al., 1992). This moderate catalytic power seems consistent with a mechanism based on preferential stabilization of a transition state by nonbonded interactions.

Comparison of the trajectories for the *twisted* and *cis* conformations allows identification of key interactions for the catalysis. An important contribution comes from the hydrophobicity of the active site, which implies that the isomerization takes place in a less polar environment than water. Experimental and theoretical studies (Drakenberg et al., 1972; Duffy et al., 1992) have demonstrated that the amide isomerization is accelerated by about 2 kcal/mol in nonpolar solvents compared to water. Thus, about one-third of the catalytic power of the enzyme can be explained by its ability to sequester the peptide in a hydrophobic pocket. Consistently, the active site of cyclophilin also features a large number of hydrophobic groups (Ke et al., 1991, 1993), suggesting that the hydrophobic enhancement could be a common feature of the mechanism of catalysis by PPIs.

In addition to the environmental effect there are specific nonbonded interactions that preferentially stabilize the transition state. One that is probably key is the interaction between the C=O group of Ala3 and the Asp^{37} side chain. In the *cis* conformation the C=O bond is oriented with the oxygen pointing to the carboxylate of Asp^{37}, which leads to an unfavorable charge–dipole interaction. However, in the transition state, when the peptide is *twisted*, the carbonyl carbon of the C=O (Ala3) is closer to the carboxylate of Asp^{37} than the oxygen, leading to a favorable charge–dipole interaction. It is notable that due to the effect of Asp^{37} the carbonyl oxygen of Ala3 in the *twisted* form is in a position which resembles more closely the position of the trans amide

oxygen of FK506 or rapamycin than the position of the keto oxygen. This result is consistent with the fact that the keto oxygen of FK506 is not very important for binding of the drugs to FKBP (Emmer & Weber-Roth, 1992). Thus, the view that the keto amide functionality makes FK506 and rapamycin "twisted amide surrogates" is not supported (Rosen et al., 1990).

Preferential stabilization of the *twisted* over the *cis* conformation also likely comes from aryl interactions with the carbonyl oxygen of Ala3. These interactions are present in both conformations, but are more common in the *twisted* form than in the *cis*. Better hydration of the bound *twisted* peptide might be an additional contributor to the catalysis, since water bridges between peptide and protein are more abundant (1.5 versus 0.7) for the *twisted* conformation than for the *cis*. A water molecule that may be catalytically relevant is bound during the last part of the MD of the *twisted* conformation to the carbonyl oxygen of Ala3 and to the hydroxyl oxygen of Tyr^{82}. It is worth noting that very recent X-ray data on a cyclophilin–peptide complex (Ke et al., 1993) also suggest a catalytic role for a water molecule hydrogen bonded to the carbonyl oxygen of the *twisted* peptide bond.

Overall, the results identify several residues that appear to be important for the catalysis. The proposed residues are obvious targets for experimental mutation. Trp^{59} is certainly important since it defines the bottom of the active site, and contacts the proline ring. Asp^{37} is also important; it is involved in hydrogen bonds with the amino groups of Ala2 and Ala3, and it is responsible for a charge-dipole interaction with the C=O of Ala3 that might be key for the catalysis. Both Tyr^{26} and Tyr^{82} may have relevance in the catalysis due to their role in aryl interactions and water bridges, though direct interactions of these residues with the peptide did not occur during the simulations. Phe^{36} and Phe^{99} probably play a lesser role due to their interactions with O(Ala3), but the aryl interactions are only one among the different nonbonded interactions stabilizing preferentially the transition state. Glu^{54} and Ile^{56}, which are hydrogen bonded to the inhibitors of FKBP (van Duyne et al., 1991a,b), are often water-bridge to the peptide. However, they are not usually involved in direct hydrogen-bond interactions, which suggests that they are not essential. His^{87} has only a moderate role in the peptide–protein interactions, and it is not expected to be a key group for catalysis, as might also be inferred from the pH independence of the enzyme (Harrison & Stein, 1990). Finally, other hydrophobic residues have an unspecific and cumulative effect in increasing the hydrophobicity of the active site, which aids the catalysis.

In summary, the simulations suggest a mechanism of catalysis where the enhancement in isomerization rate comes from the combination of nonspecific stabilization of the transition state by the hydrophobic environment and the sum of different specific interactions, like the Asp^{37}-C=O (Ala3) charge–dipole interactions, aryl interactions, water bridges, and the N–H(Phe5)–N(Pro4) interaction. Hence, many groups contribute to the catalysis, Asp^{37} and Trp^{59} appearing to be the most significant.

Free energy perturbation calculations were used to determine whether or not the model was able to reproduce the trend in experimental data for $\Delta G^{\ddagger}$ of isomerization of X-Ala-Ala-Pro-Phe-Y and X-Ala-Gly-Pro-Phe-Y. This test is challenging considering the difficulties in carrying out free energy perturbation calculations on large systems like proteins. Accord between theoretical and experimental results would support the proper placements of the methyl group of Ala3 in the active site for both conformations. Considering the conformational restrictions for the peptide inside the active site, proper location of the methyl group of Ala3 virtually ensures that the N(Pro)–CO(Ala3) subunit is properly located, which anchors most of the remaining peptide. The FEP calculations predict that the $\Delta G^{\ddagger}$ for the Ala(P1) peptide is 1.6 ± 0.2 kcal/mol smaller than that for the Gly(P1) peptide, while the experimental k_{cat} data for Ala(P1) and Gly(P1) peptides indicate a difference between 1.9 kcal/mol (Albers et al., 1990) and 3.9 kcal/mol (Park et al., 1992). Considering the uncertainties in the experimental data and calculations, the level of agreement is encouraging.

Additional support for the proposed models can be obtained from binding data for the *cis* peptide. The free energy difference in binding ($\Delta\Delta G_{bind}$) between Ala(P1) and Gly(P1) was computed from the difference between the free energy changes in the mutation from Ala → Gly in the protein complex (ΔG_{mut}^{prot}) and in water (ΔG_{mut}^{water}). The ΔG_{mut}^{prot} and ΔG_{mut}^{water} values from the FEP calculations are –0.2 (±0.1) kcal/mol and +0.15 (±0.1) kcal/mol respectively. The latter value, although not directly comparable due to the inclusion of intramolecular contributions, agrees well with a generic experimental difference in free energies of hydration for Ala and Gly side chains (+0.42 kcal/mol from Wolfenden et al. (1981)). Combination of the two computed numbers leads to a $\Delta\Delta G$ of binding of +0.35 kcal/mol, favoring the binding of the Gly(P1) peptide. This theoretical estimate (T = 298 K) compares well with the value of +0.62 kcal/mol (T = 278 K) that can be obtained from experimental K_m values (Parker et al., 1992) on the analogous Suc, pNA-capped peptides. Thus, the FEP results with the present structures show qualitative accord with the changes observed in both binding and catalysis upon mutation of the P1 residue from Ala to Gly.

In this paper, molecular dynamics results have been presented on the isomerization mechanism of FKBP. The resultant model is remarkably consistent with experimental data, and is open to experimental testing. Prediction of the binding conformation of a conformationally flexible peptide is clearly difficult. The results presented here appear to have clarified the mechanism of a key enzymatic process for protein folding and may also be useful in considering the design of new ligands for FKBP.

ACKNOWLEDGMENT

Gratitude is expressed to Dr. Ellen Laird, Michelle Lamb, and Professor Stuart L. Schreiber for continuing discussions. We also thank Professor John C. Clardy for the X-ray coordinates of the FKBP-rapamycin complex.

REFERENCES

Albers, M. W., Walsh, C. T., & Schreiber, S. L. (1990) *J. Org. Chem. 55*, 4984.

Bächinger, H. P. (1987) *J. Biol. Chem. 262*, 17144.

Bierer, B. E., Mattila, P. S., Standaert, R. F., Herzenberg, L. A., Burakoff, S. J., Crabtree, G., & Schreiber, S. L. (1990a) *Proc. Natl. Acad. Sci. U.S.A. 87*, 9231.

Bierer, B. E., Somers, P. K., Wandless, T J., Burakoff, S. J., & Schreiber, S. L. (1990b) *Science 250*, 556.

Drakenberg, T., & Forsen, S. (1971) *J. Chem. Soc., Chem. Commun.* 1404.

Drakenberg, T., Dahlqvist, K.-I., & Forsen, S. (1971) *J. Phys. Chem. 76*, 2178.

Duffy, E. M., Severance, D. L., & Jorgensen, W. L. (1992) *J. Am. Chem. Soc. 114*, 7535.

Emmer, G., & Weber-Roth, S. (1992) *Tetrahedron 48*, 5861.

Fischer, G., & Bang, H. (1985) *Biochim. Biophys. Acta 828*, 39.
Fischer, G., Bang, H., & Mech, C. (1984) *Biomed. Biochim. Acta 43*, 1101.
Fischer, G., Wittmann-Liebold, B., Lang, K., Kiefhaber, T., & Schmid, F. X. (1989a) *Nature 337*, 476.
Fischer, G., Berger, E., & Bang, H. (1989b) *FEBS Lett. 250*, 267.
Harding, M. W., Galat, A., Uehling, D. E., & Schreiber, S. L. (1989) *Nature 341*, 758.
Harrison, R. K., & Stein, R. L. (1990) *Biochemistry 28*, 1684.
Harrison, R. K., & Stein, R. L. (1992) *J. Am. Chem. Soc. 114*, 3464.
Jackson, S. E., & Fersht, A. R. (1991) *Biochemistry 30*, 10436.
Jorgensen, W. L., & Tirado-Rives, J. (1988) *J. Am. Chem. Soc. 110*, 1657.
Jorgensen, W. L., & Severance, D. L. (1990) *J. Am. Chem. Soc. 114*, 3464.
Jorgensen, W. L., Chandrasekhar, J., Madura, J. D., Impey, R. L., & Klein, M. (1983) *J. Chem. Phys. 79*, 926.
Ke, H., Zydowsky, L. D., Liu, J., & Walsh, C. T. (1991) *Proc. Natl. Acad. Sci. U.S.A. 88*, 9483.
Ke, H., Mayrose, D., & Cao, W. (1993) *Proc. Natl. Acad. Sci. U.S.A. 90*, 3324.
Kofron, J. L., Kuzmic, P., Kishore, I., Colon-Bonilla, E., & Rich, D. H. (1991) *Biochemistry 30*, 6127.
Lang, K., Schmid, F. X., & Fischer, G. (1987) *Nature 329*, 268.
Larive, C. K., & Rabenstein, D. L. (1993) *J. Am. Chem. Soc. 115*, 2833.
Meadows, R. P., Nettesheim, D. G., Xu, R. X., Olejniczak, E. T., Petros, A. M., Holzman, T. F., Severin, J., Gubbins, E., Smith, H., & Fesik, S. W. (1993) *Biochemistry 32*, 754.
Michnick, S. W., Rosen, M. K., Wandless, T. J., Karplus, M., & Schreiber, S. L. (1991) *Science 252*, 836.
Park, S. T., Aldape, R. A., Futer, O., DeCenzo, M. T., & Livingston, D. J. (1992) *J. Biol. Chem. 267*, 3316.
Pearlman, D. A., Case, D. A., Caldwell, J. C., Seibel, G. L., Singh, U. C., Weiner, P., & Kollman, P. A. (1991) *AMBER 4.0*, University of California, San Francisco.
Rosen, M. K., & Schreiber, S. L. (1992) *Angew. Chem., Int. Ed. Engl. 31*, 384.
Rosen, M. K., Standaert, R. F., Galat, A., Nakatsuka, M., & Schreiber, S. L. (1990) *Science 248*, 863.
Ryckaert, J. P., Ciccote, G., & Berendsen, J. C. (1977) *J. Comp. Phys. 23*, 327.
Schreiber, S. L. (1991) *Science 251*, 283.
Standaert, R. F., Galat, A., Verdine, G. L., & Schreiber, S. L. (1990) *Nature 346*, 671.
Takahashi, N. T., Hayano, T., & Suzuki, M. (1989) *Nature 337*, 473.
van Duyne, G. D., Standaert, R. E., Karplus, P. A., Schreiber, S. L., & Clardy, J. C. (1991a) *Science 252*, 839.
van Duyne, G. D., Standaert, R. F., Schreiber, S. L., & Clardy, J. C. (1991b) *J. Am. Chem. Soc. 113*, 7433.
Weiner, S. J., Kollman, P. A., Case, D. A., Singh, U. C., Ghio, C., Alagona, G., Profeta, S., & Weiner, P. (1984) *J. Am. Chem. Soc. 106*, 765.
Zwanzig, R. W. (1954) *J. Chem. Phys. 22*, 1420.